CHAPTER V

FABRICATION AND EVALUATION OF POLYCAPROLACTONE-POLY(HYDROXYBUTYRATE) OR POLY(3-HYDROXYBUTYRATE-CO-3-HYDROXYVALERATE) DUAL-LEACHED POROUS SCAFFOLDS FOR BONE TISSUE ENGINEERING APPLICATIONS

5.1 Abstract

Polycaprolactone(PCL) blend with poly(hydroxybutyrate)(PHB) or poly(3-hydroxybutyrate-co-3-hydroxyvalerate)(PHBV) dual leached scaffolds were prepared by using solvent casting and salt particulate leaching with polymer leaching technique. Well defined and interconnected pores were detected by scanning electron microscope (SEM) analysis. The blending of the PHB and PHBV in PCL scaffolds resulted in decrease porosities of the scaffolds and, the water absorption capacities of the scaffolds also decreased. The compressive modulus of the PCL-PHB and PCL-PHBV dual-leached scaffolds was greatly increased by the blending of PHB or PHBV matrix. An indirect cytotoxicity evaluation of all PCL dual-leached scaffolds with mouse fibroblastic cells (L929) and mouse calvaria-derived pre-osteoblastic cell (MC3T3-E1) indicated PCL-PHB and PCL-PHBV dual-leached scaffolds were posed as nontoxic to cells. The ability to support mouse calvaria-derived pre-osteoblastic cell (MC3T3-E1) attachment, proliferation, differentiation, and mineralization were also evaluated. The viability of cells on PCL-PHB, and PCL-PHBV dual-leached scaffolds were significantly higher than that on tissue-culture polystyrene plate (TCPS) and PCL scaffold at any given time, both PCL-PHB and PCL-PHBV dual-leached scaffolds supported the attachment of MC3T3-E1 at significantly higher levels to TCPS. During the proliferation period (day 1-3), all PCL-PHB and PCL-PHBV dual-leached scaffolds were able to support the proliferation of MC3T3-E1 at higher levels to that cells on TCPS and PCL scaffolds. For mineralization, cells cultured on surfaces of PCL-PHB and PCL-PHBV dual-leached scaffolds showed higher mineral deposition than on TCPS and PCL scaffold.
(Key-words: Scaffold, PCL, Solvent Casting/Particulate Leaching Method, PHB, PHBV)

5.2 Introduction

Tissue engineering applies methods from materials engineering and life science to create artificial constructs for regeneration of new tissue. With tissue engineering, we can create biological substitutes to repair or replace failing organs or tissues. The task of tissue engineering demands a combination of molecular biology and materials engineering, since in many applications a scaffold is needed to provide a temporary artificial matrix for cell seeding. [1]

Polymeric scaffolds play a pivotal role in tissue engineering through cell seeding, proliferation, and new tissue formation in three dimensions, showing great promise in the research of engineering a variety of tissues. [2-5] Interconnected porous architecture, sufficient porosity, appropriate mechanical properties, suitable degradation rate, biocompatibility and good cell attachment properties are the major requirements of an ideal scaffold for bone tissue engineering applications. [6-8]

As a consequence, the scaffold fabrication method should allow for the control of its pore size and shape and should enhance the maintenance of its mechanical properties and biocompatibility. [9-10] During the past year, many techniques have been applied for making porous scaffolds. Among the most popular are particulate leaching , temperature-induced phase separation , phase inversion in the presence of a liquid non-solvent , emulsion freeze-drying , electrospinning, and rapid prototyping. [11-12] Solvent casting of biocomposite scaffolds involves the dissolution of the polymer in an organic solvent, mixing with ceramic granules, and casting the solution into a predefined 3D mould. The solvent is subsequently allowed to evaporate. [13- 14]

For tissue engineering applications, aliphatic polyesters, such as poly(L-lactic acid) , polycaprolactone (PCL), poly(L-lactide/ε-caprolactone) copolymers, poly(lactide-co-glycolide), poly(3-hydroxybutyrate) and poly(3-hydroxybutyrate-co-3-hydroxyvalerate), have been widely used because of their favorable biocompatibility and degradability. [15-20] PCL is also an important member of the aliphatic polyester family. Among the biocompatible polyesters, PCL is a semicrystalline aliphatic polymer linked with ester bonds, which can be hydrolyzed in mammalian cells, metabolized via tricarboxylic acid cycle, and eliminated by

kidney. [21-23] PCL is flexible semicrystalline polymer with low melting point and exceptional blend compatibility. Therefore, PCL can be blended with other polymers to improve stress crack resistance, dye-ability, and adhesion. [24]

PHAs have been investigated as a tissue engineering scaffold due to its biocompatibility, biodegradability, and adjustable mechanical properties. [25] PHB is a biodegradable, thermoplastic polyester with high crystallinity and high melting temperature that possesses excellent mechanical strength and modulus. It is also the simplest and most common member of the PHA family. In vitro tests have shown that PHB is biocompatible to various cells including osteoblasts, fibroblasts, chondrocytes, endothelium and epithelium cells. [26] Polyhydroxybutyrate (PHB) and poly(hydroxybutyrate-cohydroxyvalerate) (PHBV) are the most well-known polymers of the polyhydroxyalkanoates family. [27] Material properties can be tailored by varying the HV content. An increase of the HV content induces an increase of the impact strength and a decrease of the melting temperature and glass transition, the crystallinity, the water permeability and the tensile strength. [28-30]

The one approach to modify and tailor material properties are by blending two polymer components either in molten or in dissolved state, aimed at superior thermal and physical properties. The fragility of PHB thus restricted its application in cartilage repair. Many research works have been made to improve the mechanical properties of PHB by blending PHB with other polymers. [31] It has been demonstrated that PHBV based blends present improved biological performances. [32]

In our previous work [33-34], the PCL and NaOH treated PCL/HA dual leached scaffolds with high porosity have been prepared by our combining modified solvent casting, particulate leaching, and polymer leaching techniques using sodium chloride and polyethylene glycol (PEG) as porogens. The purpose of this research work was to fabricate and biological evaluations of the PCL blend with PHB (PCL-PHB) and PCL blend with PHBV (PCL-PHBV) dual-leached scaffolds. Moreover, the morphology, physical and mechanical properties, and weight remaining after degradation of the PCL-PHB and PCL-PHBV dual-leached scaffolds were also investigated. For biological evaluations, the indirect cytotoxicity of L929 and MC3T3-E1 cells, MC3T3-E1 cell attachment, proliferation, and differentiation were

evaluated the potential of scaffolds for used these construct as bone scaffolding materials.

5.3 Experimental

5.3.1 Materials

Polycaprolactone (PCL; MW = 80,000 $gmol^{-1}$), poly(3-hydroxybutyrate) (PHB; MW= 300,000 $gmol^{-1}$), and poly(3-hydroxybutyrate-*co*-3-hydroxyvalerate) (PHBV; MW = 680,000 $gmol^{-1}$) were purchased from Sigma-Aldrich, USA. Chloroform was purchased from Labscan (Asia), Thailand. Polyethylene glycol (PEG; MW = 1,000 $gmol^{-1}$; Merck, Germany) and sodium chloride (Ajax Finechem, Australia) were used as porogen. All other chemicals were of analytical reagent grade and used without further purification.

5.3.2 Preparation of PCL-PHB and PCL-PHBV Scaffolds

The solvent casting, polymer leaching, and salt particulate leaching techniques were used to prepare the scaffolds. Briefly, a polymer solution was prepared by blending 10%, 20%, and 30% w/w PHB or PHBV and PCL then mix with PEG (Polymer/PEG = 1/1(w/w)) and chloroform at a concentration of 28% (w/v). The solution was then stirred at room temperature for 2-3 h. Next, NaCl particles ranging in diameter from 400-500 μm (polymer/NaCl = 1/30 (w/w)) were added. The mixture was packed into Petri dishes, creating cylindrical molds that were 1.2 mm in diameter and 0.8 mm in thickness. These molds were placed in a ventilation hood overnight to allow solvent evaporation. After evaporation, to leach out the PEG and salt particles, the constructs were immersed in deionized (DI) water for 48 h with repeated changes of the DI water every 8 h. The scaffolds were then air-dried for 24 h and vacuum-dried overnight. The resultant salt-PEG leached PCL scaffolds exhibited highly interconnected porous networks.

5.3.3 Characterization

Microstructure Observation

The pore morphology, size, distribution, and interconnectivity of the

porous scaffolds were observed using a JEOL JSM-5200 scanning electron microscope. One cylindrical scaffold was randomly selected from each group, cut with a razor blade in the middle and mounted onto a stub. These cross sections were coated with a thin film of gold using a JEOL JFC-1100E sputtering device for 5 min prior to observation by scanning electron microscopy (SEM).

Porosity, Pore Volume, and Pore Size

The porosity and pore volume of the scaffolds were determined gravimetrically, according to the following equations:

$$\text{Porosity}(\%) = \left(1 - \frac{\rho\text{scaffold}}{\rho\text{polymer}}\right) x\ 100$$

$$\text{Pore volume} = \left(\frac{1}{\rho\text{scaffold}} - \frac{1}{\rho\text{polymer}}\right) x\ 100$$

where $\rho_{polymer}$ is the density of the polymer from which the scaffolds were fabricated, and $\rho_{scaffold}$ is the apparent density of the scaffolds, determined using a Sartorius YDK01 density measurement kit. Here, ρ_{PCL} was considered to be 1.145 gcm^{-1}. Ten specimens were assessed for both porosity and pore volume, and an average value was calculated for each property. In contrast, the pore size of each scaffold was directly measured from the SEM images using a SemAfore Digital slow-scan image-recording system (version 5.0 software). At least 30 pores for each of the cross and longitudinal sections (i.e., at least 60 pores in total) were analyzed, and average values were calculated for all of the scaffolds investigated.

Water Absorption Capacity

The scaffold specimens were cut from the molds, which were created by casting in Petri dishes with a circular shape measuring 15 mm in diameter and 3 mm in height. The constructs were first dried, weighed, and individually immersed in 10 mL of 10 mM phosphate-buffered saline (PBS; pH 7.4) at room temperature. At a specified point in time, the specimens were removed from the solution, carefully placed on glass for 5 sec to remove any excess water, and weighed immediately. The amount of water retained in each scaffold was determined according to the following equation:

$$\text{Water absorption}(\%) = \frac{(Ww - Wd)}{Ww}\ x\ 100$$

where W_d and W_w are the weights of the specimen before and after submersion in the medium, respectively. This experiment was conducted in pentuplicate, and measurements were performed at different time points within a period of 7 d.

Compressive Modulus

The compressive modulus of each scaffold was determined using a universal testing machine (Lloyd LRX, UK) and a load cell of 500 N in a dry state at room temperature. The load was vertically compressed at a crosshead speed of 3 mm/min until the scaffolds were reduced to approximately 70% of the original thickness. The initial compressive modulus was then determined from the slope of the linear portion of the stress-strain curve at a compressive strain of 20%.

Degradation

The degradation of all scaffolds had been examined up to 13 weeks. Briefly, 5 scaffolds from each type of material had been separately immersed in 5 ml of 0.1M PBS, pH 7.4 with or without lipase (*Pseudomonas sp.*, 45 units/l). The samples were kept at 37°C up to 13 weeks with the replacing of new medium at every 84 hr throughout the experiment in order to keep enzymatic activity at the constant level. The samples were taken out at every 2 weeks, washed thoroughly with distilled water and dried at room temperature for 24 hr and in a vacuum for another 48 hr. The remaining weight of the scaffolds was investigated. The scaffold remaining weight was measured and calculated by the following equation.

$$\text{Remaining weight}(\%) = \frac{Wt}{Wo} \, x \, 100$$

where W_O is the initial weight and W_t is the weight of the scaffold at a single degradation time point. An average remaining weight was calculated from those of five samples in each group.

5.3.4 Biological Evaluation of PCL-PHB and PCL-PHBV Scaffolds

Cell Culturing

Mouse fibroblasts (L929) and mouse calvaria-derived pre-osteoblastic cells (MC3T3-E1) were used as reference cell lines. The L929 cells were cultured as a monolayer in Dulbecco's modified Eagle's medium (DMEM; Sigma-Aldrich, USA) supplemented with 10% fetal bovine serum (FBS; BIOCHROM AG); 1% L-

glutamine (Invitrogen); and 1% antibiotic and antimycotic formulation, containing penicillin G sodium, streptomycin sulfate, and amphotericin B (Invitrogen, USA). The MC3T3-E1 cells were cultured in Minimum Essential Medium (MEM; Hyclone, USA) with Earle's Balanced Salts and supplemented with 10% FBS (BIOCHROM AG, Germany), 1% L-glutamine (Invitrogen, USA), and 1% antibiotic and antimycotic formulation, as described above. The media were replaced every 2 days, and the cultures were maintained at 37°C in a humidified atmosphere containing 5% CO_2.

Each scaffold was cut into circular discs of approximately 15 mm in diameter, which were placed into the wells of a 24-well tissue-culture polystyrene (TCPS) plate. The discs were then sterilized in 70% ethanol for 30 min, washed with autoclaved DI water and PBS, and immersed in MEM overnight. To ensure complete contact between the scaffolds and the wells, each construct was pressed with a metal ring of approximately 12 mm in diameter.

The cultured MC3T3-E1 cells were detached using 0.25% trypsin containing 1 mM EDTA (Invitrogen, USA) and counted with a hemacytometer (Hausser Scientific, USA). The cells were then seeded on the scaffolds at a density of approximately 40,000 cells/well for the attachment and proliferation studies. Seeded, empty wells of a TCPS plate were used as a control. For the indirect cytotoxicity, alkaline phosphatase activity, and mineralization evaluations, the MC3T3-E1 cells were seeded at a density of approximately 40,000 cells/well on the scaffolds and empty wells of a TCPS plate. The culture was maintained in an incubator at 37°C with a humidified atmosphere containing 5% CO_2.

Indirect Cytotoxicity Evaluation

Two cell types were used for the cytotoxicity evaluation: 1) mouse calvaria-derived pre-osteoblastic cells (MC3T3-E1) and 2) mouse fibroblasts (L929). In particular, an indirect cytotoxicity test was conducted on TCPS wells and on PCL, PCL-10%PHB, PCL-20%PHB, PCL-30%PHB, PCL-10%PHBV, PCL-20%PHBV, and PCL-30%PHBV scaffolds. First, the extraction media were prepared by immersing the samples, which were approximately 15 mm in diameter, in serum-free medium (SFM) containing DMEM (for the L929 cells) or MEM (for the MC3T3-E1

cells), supplemented with 1% L-glutamine, 1% lactalbumin, and 1% antibiotic and antimycotic formulation, for 1, 3, or 7 days. Each of these extraction media was then used to evaluate the cytotoxicity of the scaffolds. Either the L929 cells or the MC3T3-E1 cells were cultured in the wells of a 24-well culture plate containing 10% FBS-supplemented DMEM or MEM, respectively, for 16 h to allow cell attachment to the plate. Next, the cells were starved in SFM for 24 h, after which the medium was replaced with extraction medium. After an additional 24 h of cell culture, a 3-(4,5-dimethylthiazol-2-yl)-2,5-diphenyl-tetrazolium bromide (MTT) assay was performed to quantify the number of viable cells. These experiments were conducted in triplicate.

MTT Assay

The MTT assay is based on the reduction of yellow tetrazolium salt to purple formazan crystals by dehydrogenases secreted by the mitochondria of metabolically active cells. The amount of purple formazan crystals formed is proportional to the number of viable cells. In the current study, the culture medium was first aspirated and replaced with 400 μL/well of MTT solution at 0.5 mg/mL in a 24-well culture plate. Second, each plate was incubated for 30 min at 37°C. The MTT solution was then aspirated, and 1 mL/well of dimethyl sulfoxide (DMSO) containing 125 μL/well of glycine buffer (pH 10) was added to dissolve the formazan crystals. Finally, after 5 min of rotary agitation, the absorbance of the DMSO solution at 540 nm was measured using a Thermo Spectronic Genesis10 UV/Visible spectrophotometer.

Cell Attachment and Proliferation

Cell behaviors, such as adhesion and proliferation, represent the initial phase of cell-scaffold communication, which subsequently affects cell differentiation and mineralization. In the attachment study, the MC3T3-E1 cells were allowed to adhere to the TCPS, PCL, PCL-10%PHB, PCL-20%PHB, PCL-30%PHB, PCL-10%PHBV, PCL-20%PHBV, and PCL-30%PHBV scaffolds for 4, 8 or 16 h. Each sample was then rinsed with PBS to remove unattached cells prior to morphological assessment of the adherent cells by SEM. In the proliferation study, the viability of the cells on the scaffolds was determined after 1, 2, or 3 days of cell culture by Alamar Blue Assay. These experiments were performed in triplicate.

Alamar Blue Assay

Resazurin, the active ingredient of alamarBlue reagent, is a non-toxic, cell permeable compound that is blue in color and virtually non-fluorescent. Upon entering cells, resazurin is reduced to resorufin, a compound that is red in color and highly fluorescent. Viable cells continuously convert resazurin to resorufin, increasing the overall fluorescence and color of the media surrounding cells. First, each culture medium was removed and replaced with 500 μL/well of 10% alamar blue solution for a 24-well culture plate. Secondly, the plate was incubated for 3 hours at 37 °C. Finally, the fluorescent emission intensity of the obtained solution was then measured at 585 nm, after it had been excited at 570 nm, using the microplate reader.

Morphological Observation of Cultured Cells

After removal of the culture medium, the cell-seeded scaffolds were rinsed twice with PBS and fixed in 3% glutaraldehyde solution, which was diluted from 50% glutaraldehyde solution (Sigma, USA) with PBS, at 500 μL/well. After 30 min, the wells were again rinsed with PBS. Following cell fixation, the specimens were dehydrated in ethanol solutions of varying concentrations (i.e., 30, 50, 70, 90, and 100%) for approximately 2 min at each concentration and dried in 100% hexamethyldisilazane (HMDS; Sigma, USA) for 5 min. The scaffolds were allowed to air-dry after the removal of the HMDS. The completely dry specimens were mounted on SEM stubs, coated with gold, and observed using a JEOL JSM-5200 scanning electron microscope.

Production of Alkaline Phosphatase (ALP) by Cultured Cells

The ALP activity of the MC3T3-E1 cells was measured using Alkaline Phosphate Yellow Liquid. In this reaction, ALP catalyzes the hydrolysis of the colorless organic phosphate-ester substrate *p*-nitrophenyl phosphate (pNPP) to a yellow product, p-nitrophenol, and a phosphate. In the present study, the MC3T3-E1 cells were cultured on scaffold specimens for 3, 5, or 7 days to observe the production of ALP. The specimens were then rinsed twice with PBS after the removal of the culture medium. Alkaline lysis buffer (10 mM Tris-HCl, 2 mM $MgCl_2$, and 0.1% Triton X-100, pH 10 was added at 200 μL/well, and the samples

were scraped and frozen at -20°C for at least 30 min prior to the next step. An aqueous solution of 2 mg/mL pNPP (Zymed Laboratories, USA) mixed with 0.1 M amino propanol (10 μL/well) in 2 mM $MgCl_2$ (100 μL/well) at a pH 10.5 was prepared and added to the specimens (110 μL/well), followed by incubation at 37°C for 15 min. The reaction was stopped by adding 900 μL/well of 50 mM NaOH, and the extracted solution was transferred to a cuvette and placed in the UV-visible spectrophotometer, from which the absorbance at 410 nm was measured. The amount of ALP was then calculated using a standard curve. To determine the ALP activity, the amount of ALP was normalized to the total amount of protein synthesized.

In the protein assay, the samples were treated in the same manner as in the ALP assay up to the point at which the specimens were frozen. After freezing, bicinchoninic acid (BCA; Pierce Biotechnology, USA) solution was added to the scaffolds, which were then incubated at 37°C for 15 min. The absorbance of the medium was measured at 562 nm using the UV-visible spectrophotometer, and the total amount of protein was calculated using a standard curve.

Mineralization Analysis

Alizarin Red S dye binds selectively to calcium salts and is widely used for mineral staining (i.e., the staining product is an Alizarin Red S calcium chelating product). The isolated MC3T3-E1 cells were plated on 24-well plates at 40,000 cells/well and maintained in culture medium. After 24 h, the cultures were treated with medium supplemented with 50 μg/ml ascorbic acid (Sigma, USA), 5 mM β-glycerophosphate (Sigma, USA), and 0.2 μg/mL dexamethasone (Sigma, USA), which was replaced every 2 days. After 14 and 21 days of treatment, the cells were washed with PBS, fixed in ice-cold absolute methanol for 10 min, and stained with 1% Alizarin Red S in DI water (Sigma, USA) at pH 4.2 for 2-3 min. After removing the alizarin red S solution, the cells were rinsed with DI water and dried at room temperature. The images of each culture were captured, and the stain was extracted using 10% cetylpyridinium chloride (Sigma, USA) in 10 mM sodium phosphate for 1 h. The absorbance of the collected dye was read at 570 nm using a UV-visible spectrophotometer (Thermo Spectronics Genesis10).

5.3.5 Statistical Analysis

All of the values were expressed as the mean ± standard deviation. Statistical analyses of the different data groups were performed by one-way analysis of variance (ANOVA), along with the least-significant difference (LSD) test, using SPSS software version 11.5. Values with $p < 0.05$ were considered statistically significant.

5.4 Results and Discussion

5.4.1 Characterization of PCL, PCL-PHB and PCL-PHBV Scaffolds

Microstructure Observation

Table 5.1 show the SEM micrographs of microporous scaffolds formed by PEG and NaCl salt blend in PCL, PCL-PHB, and PCL-PHBV matrix following by leaching in aqueous medium. Well defined and interconnected pores, detected by SEM analysis of PCL, PCL-PHB, and PCL-PHBV dual-leached scaffolds, resulted from the use of both salt and PEG. The interconnected pores were formed in scaffolds after PEG was leached out. SEM images of PCL-PHB and PCL-PHBV dual-leached scaffolds showed that both scaffold types exhibited a similar porous structure while PCL dual-leached scaffold exhibited a difference porous structure.

Table 5.2 show the pore size of PCL, PCL-PHB and PCL-PHBV dual-leached scaffolds. The pore dimensions of the PCL, PCL-10%PHB, PCL-20%PHB, PCL-30%PHB, PCL-10%PHBV, PCL-20%PHBV, and PCL-30%PHBV dual-leached scaffolds are in the range of 452±31, 382±20, 350±21, 376±36, 367±29, 385±26, and 373±32 respectively. The size of pores in PCL dual-leached scaffold was larger than PCL-PHB and PCL-PHBV dual-leached scaffolds and more interconnected channels were distributed throughout the PCL dual-leached scaffold. SEM images revealed that the PCL-PHB and PCL-PHBV dual-leached scaffolds presented with decreased microporosity when compared to PCL dual-leached scaffold, indicating that blending of PHB and PHBV affected the processing of the scaffold. Moreover they also showed the preservation of macropore interconnectivity and the presence of PHB and PHBV matrix distributed within the PCL matrix.

Table 5.1 SEM images at 50x, and 200x magnification illustrating the microstructures of the PCL, the PCL-PHB, and PCL-PHBV dual-leached scaffolds

Scaffolds	Magnification	
	50x	200x
PCL	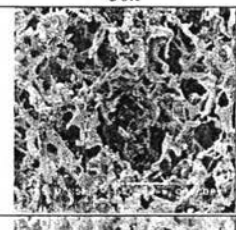	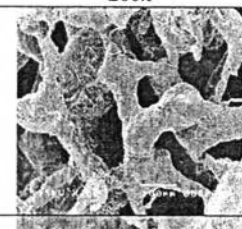
PCL-10% PHB	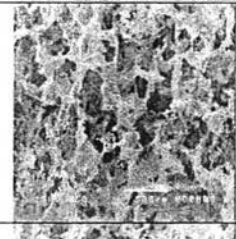	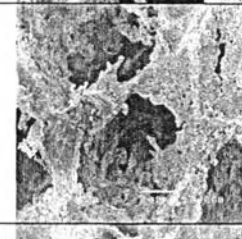
PCL-20% PHB	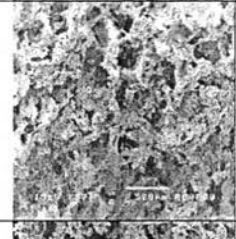	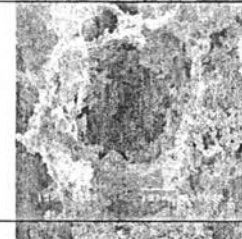
PCL-30% PHB	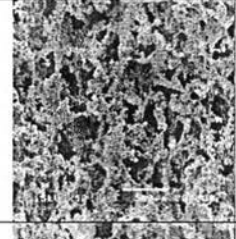	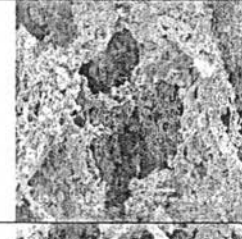
PCL-10% PHBV	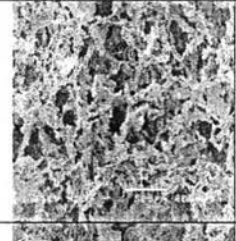	
PCL-20% PHBV	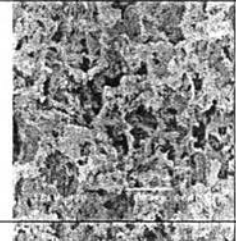	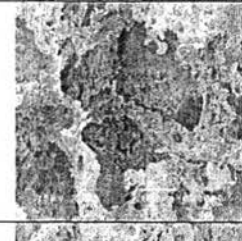
PCL-30% PHBV	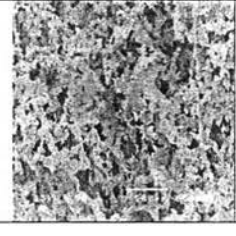	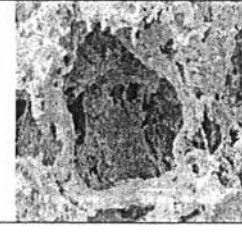

Table 5.2 Density, percentage of porosity, pore volume, and compressive modulus of the PCL, PCL-PHB and PCL-PHBV dual-leached scaffolds: a,b,c,d, e , f , g are significantly different at $p < 0.05$ for an individual feature; *one way ANOVA with Tukey HSD, and n = 10 for porosity pore volume. n = 30 for pore size

Scaffolds	Density* (g/cm^3)	Porosity* (%)	Pore volume* (cm^3/g)	Pore size (μm)	Compressive modulus (kPa)
PCL	0.0853±0.0063 b,c,d,e,f,g	92.55±0.55 a,c,d,e,f,g	10.9104±0.8774 a,c,d,e,f,g	452±31	57.7±8.2
PCL-10% PHB	0.1876±0.0464 a,d	83.61±4.05 a,d	4.7761±1.5218 a,d	382±20	287±6.9
PCL-20% PHB	0.1540±0.0433 a,e	86.55±3.78 a,e	6.1134±2.0485 a	350±21	735±4.5
PCL-30% PHB	0.1347±0.0307 a,b,e	88.24±2.68 a,b,e	6.9269±1.8898 a,b,e,	376±36	1,223±1.4
PCL-10% PHBV	0.2129±0.0605 a,c,d,f,g	81.41±5.29 a,c,e,f,g	4.1519±1.3218 a,d,g	367±29	951±1.3
PCL-20% PHBV	0.1512±0.0238 a,e	86.80±2.08 a,e	5.8870±1.0363 a	385±26	1,708±8.0
PCL-30% PHBV	0.1375±0.0148 a,e	87.99±1.29 a,e	6.4688±0.7454 a,e	373±32	1,861±1.0

Density, Porosity, and Pore Volume

The density, the porosity, and the pore volume of the PCL, PCL-PHB, and PCL-PHBV scaffolds that had been prepared as a function of the PHB or PHBV content (i.e., 10-30% w/w) are shown in table 5.2.

The porosity of the PCL scaffolds was 92.55% on average, whereas the porosity of the PCL-PHB and PCL-PHBV scaffolds ranged from 83.61-88.24% and 81.41-87.99% on average (n = 10). In particular, the porosity decreased from approximately 92.55% for the PCL scaffolds to approximately 83.61% for the PCL-10%PHB scaffolds, 86.55% for the PCL-20%PHB scaffolds, 88.24% for the PCL-30%PHB scaffolds, 81.41% for the PCL-10%PHBV scaffolds, 86.80% for the PCL-20%PHBV scaffolds, and 87.99% for the PCL-30%PHBV scaffolds.

The density of PCL scaffold was 0.0853 g/cm^3 and the density of PCL-PHB and PCL-PHBV scaffolds were 0.1347-0.1876 g/cm^3 and 0.1375-0.2129 g/cm^3. Whereas the density value increased with the blending of PHB or PHBV, that is, from about 0.0853 g/cm^3 on average for the PCL dual-leached scaffold to about

0.1876 g/cm^3 on average for the PCL-10%PHB scaffold, 0.1540 g/cm^3 on average for the PCL-20%PHB scaffold, 0.1347 g/cm^3 on average for the PCL-30%PHB scaffold, 0.2129 g/cm^3 on average for the PCL-10%PHBV scaffold, 0.1512g/cm^3 on average for the PCL-20%PHBV scaffold, and 0.1375 g/cm^3 on average for the PCL-30%PHBV scaffold (n=10). Specially, pore volume decreased from 10.9104 cm^3g^{-1} for PCL scaffold to 4.7761 cm^3g^{-1} PCL-10%PHB scaffold, 6.1134 cm^3g^{-1} PCL-20%PHB scaffold, 6.9269 cm^3g^{-1} PCL-30%PHB scaffold, 4.1519 cm^3g^{-1} PCL-10%PHBV scaffold, 5.8870 cm^3g^{-1} PCL-20%PHBV scaffold, and 6.4688 cm^3g^{-1} PCL-30%PHBV scaffold. The pore volume increased with an increased the porosity. The blending of PHB or PHBV increased the density but decreased the porosity values of the scaffolds. The porosity values decrease with blending of PHB or PHBV because the PHB or PHBV matrix might occupy the free space available in pores.

Table 5.2 Density, percentage of porosity, pore volume, and compressive modulus of the PCL, PCL-PHB and PCL-PHBV dual-leached scaffolds: a,b,c,d, e , f , g are significantly different at $p < 0.05$ for an individual feature; *one way ANOVA with Tukey HSD, and n = 10 for porosity pore volume. n = 30 for pore size

Scaffolds	Density* (g/cm^3)	Porosity* (%)	Pore volume* (cm^3/g)	Pore size (μm)	Compressive modulus (kPa)
PCL	0.0853±0.0063 b,c,d,e,f,g	92.55±0.55 a,c,d,e,f ,g	10.9104±0.8774 a,c,d,e,f,g	452±31	57.7±8.2
PCL-10% PHB	0.1876±0.0464 a,d	83.61±4.05 a,d	4.7761±1.5218 a, d	382±20	287±6.9
PCL-20% PHB	0.1540±0.0433 a,e	86.55±3.78 a,e	6.1134±2.0485 a	350±21	735±4.5
PCL-30% PHB	0.1347±0.0307 a,b,e	88.24±2.68 a,b,e	6.9269±1.8898 a, b,e,	376±36	1,223±1.4
PCL-10% PHBV	0.2129±0.0605 a,c,d,f,g	81.41±5.29 a,c,e,f,g	4.1519±1.3218 a, d,g	367±29	951±1.3
PCL-20% PHBV	0.1512±0.0238 a,e	86.80±2.08 a,e	5.8870±1.0363 a	385±26	1,708±8.0
PCL-30% PHBV	0.1375±0.0148 a,e	87.99±1.29 a,e	6.4688±0.7454 a, e	373±32	1,861±1.0

Water Absorption Capacity

Figure 5.1 illustrates the water absorption capacities of the PCL, PCL-PHB and PCL-PHBV scaffolds in 0.1 M PBS at room temperature within 3 days. The water absorption rate increased rapidly in the early 1 h and slightly increased in 3 d for PCL scaffolds. The water absorption rate of PCL-PHB rapidly increased in 12 h, and slightly increased in 3 d while the water absorption rate of PCL-PHBV increased rapidly in 12 h, and increased continuously in 3 d. The water absorption capacities of PCL-PHB and PCL-PHBV scaffolds were lower than the water absorption capacities of PCL scaffold at the any given time point. The water absorption capacities of PCL-PHB scaffold were lower than the water absorption capacities of PCL-PHBV scaffolds at the early time point and were similar to the water absorption capacities of PCL-PHBV scaffold at 3d. The blending of the PHB and PHBV in PCL scaffolds resulted in decrease porosities of the scaffolds and, the water absorption capacities of the scaffolds also decreased.

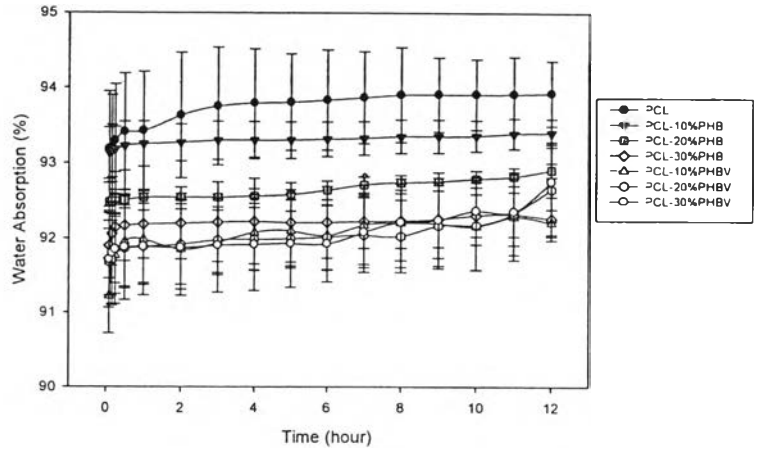

(a)

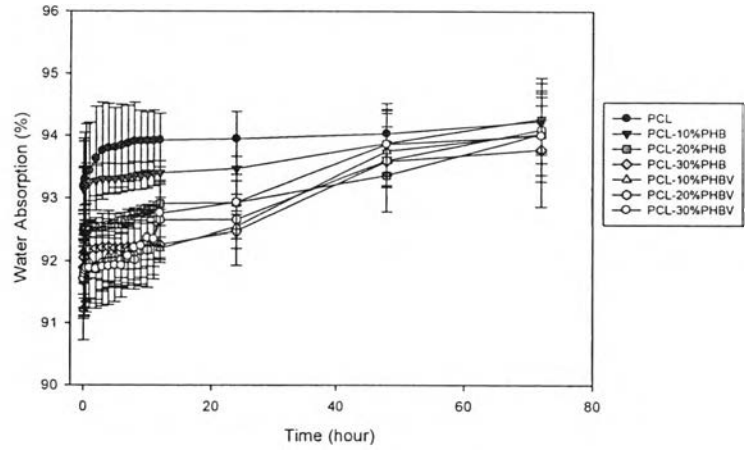

(b)

Figure 5.1 **(a)** Water absorption capacity of PCL, PCL-PHB, and PCL-PHBV dual-leached scaffolds in 0.1 M PBS at room temperature over 12 hours. **(b)** Water absorption capacity of PCL, PCL-PHB, and PCL-PHBV dual-leached scaffolds in 0.1 M PBS at room temperature over 3 days.

Compressive Modulus

The mechanical properties of porous scaffolds are evaluated by compressive tests. The compressive modulus of PCL, PCL-PHB and PCL-PHBV scaffolds are shown in table 5.2. Compared with PCL scaffold, PCL-PHB and PCL-PHBV scaffolds exhibit higher compressive modulus. The compressive modulus increased from ~ 58 MPa for the PCL scaffold to 287,735, 1223, 951, 1708, and 1861 kPa for PCL-10%PHB, PCL-20%PHB, PCL-30%PHB, PCL-10%PHBV, PCL-20%PHBV, and PCL-30%PHBV scaffolds, respectively. The blending of the PHB and PHBV in PCL scaffolds resulted in an increase in compressive properties.

Table 5.2 Density, percentage of porosity, pore volume, and compressive modulus of the PCL, PCL-PHB and PCL-PHBV dual-leached scaffolds: a,b,c,d, e , f , g are significantly different at $p < 0.05$ for an individual feature; *one way ANOVA with Tukey HSD, and n = 10 for porosity pore volume. n = 30 for pore size

Scaffolds	Density* (g/cm^3)	Porosity* (%)	Pore volume* (cm^3/g)	Pore size (μm)	Compressive modulus (kPa)
PCL	0.0853±0.0063 b,c,d,e,f,g	92.55±0.55 a,c,d,e,f,g	10.9104±0.8774 a,c,d,e,f,g	452±31	57.7±8.2
PCL-10% PHB	0.1876±0.0464 a,d	83.61±4.05 a,d	4.7761±1.5218 a,d	382±20	287±6.9
PCL-20% PHB	0.1540±0.0433 a,e	86.55±3.78 a,e	6.1134±2.0485 a	350±21	735±4.5
PCL-30% PHB	0.1347±0.0307 a,b,e	88.24±2.68 a,b,e	6.9269±1.8898 a,b,e	376±36	1,223±1.4
PCL-10% PHBV	0.2129±0.0605 a,c,d,f,g	81.41±5.29 a,c,e,f,g	4.1519±1.3218 a,d,g	367±29	951±1.3
PCL-20% PHBV	0.1512±0.0238 a,e	86.80±2.08 a,e	5.8870±1.0363 a	385±26	1,708±8.0
PCL-30% PHBV	0.1375±0.0148 a,e	87.99±1.29 a,e	6.4688±0.7454 a,e	373±32	1,861±1.0

Remaining weight after degradation

Figure 5.2 shows the remaining weight of the scaffolds after degrading in the absence and presence of the enzyme lipase in 0.1 M PBS pH 7.4 at 37°C for 13 weeks. In the absence of lipase (fig 5.2 (a)), the PCL-10%PHB, PCL-20%PHB, and PCL-30%PHB dual leached scaffolds did not show the rapidly change of remaining weight while the PCL scaffolds did not show the rapidly change of remaining weight until the end of 13 weeks. Whereas the remaining weight of PCL-10%PHBV, PCL-20%PHBV, and PCL-30%PHBV scaffolds were rapidly significant drop and remaining weights were only 66.2%, 66.1,% and 62.6%, respectively. It can be said that the PCL-PHBV scaffolds also showed high water uptake which is another factor in the hydrolytic degradation due to water could lead to swelling of the polymer and thus facilitate degradation. The biodegradability of these dual leached scaffolds in the absence lipase solution can be rank as follows: PCL-30%PHBV > PCL-20%PHBV > PCL-10%PHBV > PCL > PCL-30%PHB > PCL-20%PHB > PCL-10%PHB. In the presence of lipase (figure 5.2 (b)), it was clearly observed that the remaining weight of PCL, PCL-PHB and PCL-PHBV dual leached scaffolds were much decreasing compare to the absence of lipase condition. For PCL, PCL-10%PHB, PCL-20%PHB, PCL-30%PHB, PCL-10%PHBV, PCL20%PHBV, and PCL-30%PHBV dual leached scaffolds, the percentage of decreasing weight were 80.0%, 75.6%, 80.5%, 81.8%, 64.3%, 58.4%, and 62.7%, respectively. The activity of this enzyme lipase exhibited an effect to PCL, PCL-PHB, and PCL-PHBV dual leached scaffolds. Additionally, the degradation profiles of PCL and PCL-PHB dual leached scaffolds were similar; they revealed the gradual decreasing of weight in 13 weeks. Whereas the degradation rate of PCL-10%PHBV and PCL-20%PHBV dual leached scaffolds tented to decrease rapidly in the 13 weeks and the degradation rate of PCL-20%PHBV dual leached scaffold tended to decrease rapidly and dramatically drop of weight after 9 weeks. The biodegradability of these polyester scaffolds in lipase solution can be rank as follows: PCL-20%PHBV > PCL-30%PHBV > PCL-10%PHBV >PCL-10% PHB > PCL > PCL-20%PHB > PCL-30%PHB.

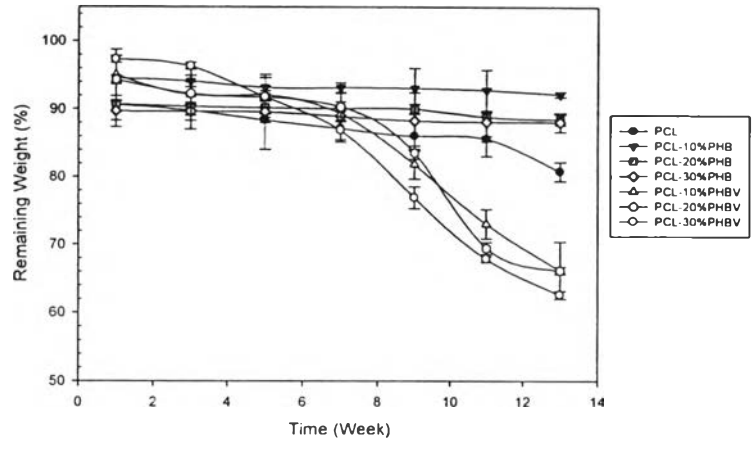

(a)

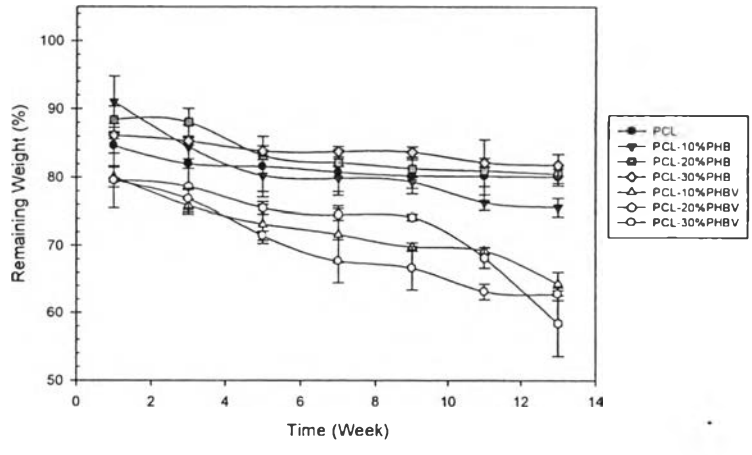

(b)

Figure 5.2 Remaining weight of the scaffolds after 13 weeks degradation in 0.1 M PBS containing (a) without lipase, (b) with lipase.

5.4.2 Biological Evaluation of PCL, PCL-PHB and PCL-PHBV Scaffolds

Indirect Cytotoxicity Evaluation

An Indirect cytotoxicity evaluation was conducted on PCL, PCL-PHB, and PCL-PHBV dual-leached scaffolds by using mouse calvaria-derived preosteoblastic cells(MC3T3-E1) and mouse fibroblasts cells (L929). Even though we were interested in using the obtained scaffolds as potential bone scaffolds, it was mandatory to test the materials with L929 just to comply with the ISO10993-5 standard test method. For both types of cells, about 40,000 cells/well were seeded in

empty wells of TCPS. Figure 5.3 (a) and 5.3 (b) show the viability of the cells obtained from MTT assay after the cells had been cultured with the 1, 3, 7 day-extraction media from scaffolds as compared with that obtained after the cells had been cultured with the fresh SFM(control TCPS). The viability of the cells was reported as the percentage with respect to that of the TCPS. Evidently, the viability ratio of cells that had been cultured with all of extraction media from PCL, PCL-PHB, and PCL-PHBV dual-leached scaffolds (and with control TCPS) were greater than 80%. These results could be suggested that all types of PCL-PHB and PCL-PHBV dual-leached scaffolds posed no threats to the cells.

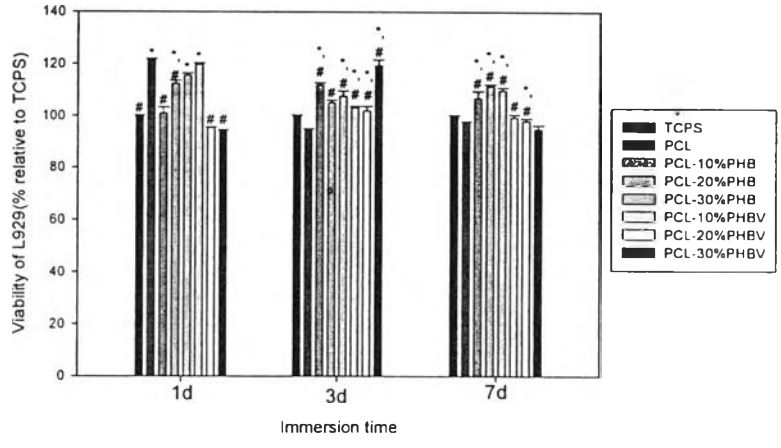

(a)

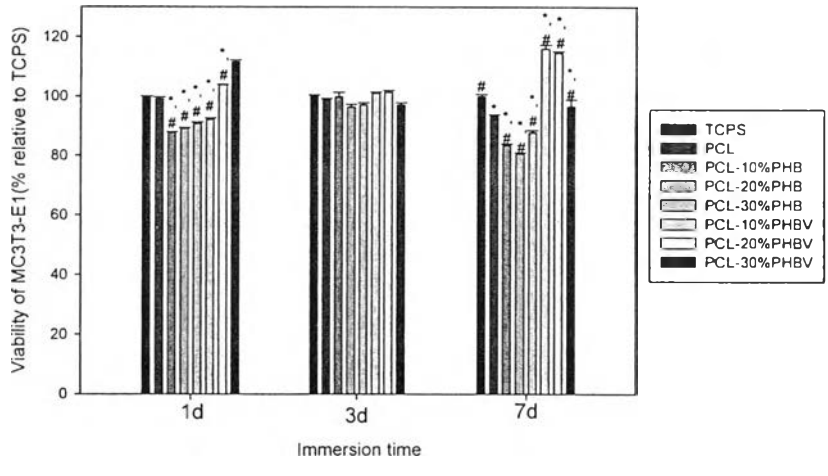

(b)

Figure 5.3 Indirect cytotoxic evaluation of TCPS, PCL, PCL-10%PHB, PCL-20%PHB, PCL-30%PHB, PCL-10%PHBV, PCL-20%PHBV and PCL-30%PHBV dual-leached scaffolds, based on the viability of (a) mouse fibroblasts (L929) and (b) pre-osteoblasts (MC3T3-E1) that were cultured with the extraction medium from each scaffold. Cell viability was tested using cells that had been cultured with their respective culture media each day as a function of the incubation time of the extraction and the culture media of 1, 3, or 7 days. Statistical significance: $^{*}p < 0.05$ compared with control and $^{\#}p < 0.05$ compared to the PCL scaffolds at any given time point.

Cell Attachment and Cell Proliferation

The potential for the PCL-PHB and PCL-PHBV dual-leached scaffolds in supporting both the attachment and the proliferation of bone cells were assessed with MC3T3-E1. The cells were either seeded or cultured on the surfaces of the PCL, PCL-PHB, and PCL-PHBV dual-leached scaffolds and TCPS (control) for 4, 8 16 h and 1, 2, 3 day. Figure 5.4 shows the attachment of MC3T3-E1 on the surface of TCPS, the PCL, PCL-PHB, and PCL-PHBV dual-leached scaffolds on 4, 8, and 16 h after cell culturing in terms of the viability of cells (%relative to TCPS at 4 h). The viability of cells on a scaffold could be quantified by Fluorescent emission intensity from the Alarmar Blue assay. On TCPS, the number of cells increased from ~100% on 4 h after cell culture to ~133% on 16 h after cell culturing, based on the initial 40,000 cells/well of cells seeded. In comparison with the viability of cells on TCPS, the viability of cells on PCL, PCL-PHB, and PCL-PHBV dual-leached scaffolds were significantly higher at any given time point. The viability of cells on PCL-PHB dual-leached scaffold was slightly lower than that on PCL on 4 h and was significantly higher than that on PCL on 8, and 16 h. But that on PCL-PHBV dual-leached scaffold was significantly higher than that on PCL and PCL-PHB on 4, 8, and 16 h.

Figure 5.5 shows the proliferation of MC3T3-E1 on the surface of TCPS, the PCL, PCL-PHB, and PCL-PHBV dual-leached scaffolds on day 1, 2, and 3 after cell culturing in terms of the viability of cells (%relative to TCPS at day1). The viability of cells on a scaffold could be quantified by Fluorescent emission intensity from the Alarmar Blue assay. On TCPS, the number of cells increased from ~100% on day1 after cell culture to ~147% on day 3 after cell culturing, based on the initial 40,000 cells/well of cells seeded. In comparison with the viability of cells on TCPS, the viability of cells on all PCL, PCL-PHB, and PCL-PHBV dual-leached scaffolds were significantly higher at any given time point. On day 1 and 2, the viability of cell on the PCL-PHB and PCL-PHBV dual-leached scaffolds were significantly higher than that on PCL dual-leached scaffold and the viability of cell on the PCL-PHB and PCL-PHBV dual-leached scaffolds were not different. The viability of cell on the PCL-PHB and PCL-PHBV dual-leached scaffolds were greater than that on PCL dual-leached scaffold on day 3 and the viability of cell on

the PCL-10%PHB scaffolds shows the highest on day 3. For the proliferation of the cells, all PCL dual-leached scaffolds are able to support the proliferation of the cells at significantly higher levels to that on TCPS, this results could be suggested that the PCL-PHB and PCL-PHBV dual-leached scaffolds provided better support for bone cell adhesion and proliferation. The better support of the PCL-PHB and PCL-PHBV dual-leached scaffold for bone cell culture should be due to the blending of PHB or PHBV matrix in PCL dual leached scaffolds.

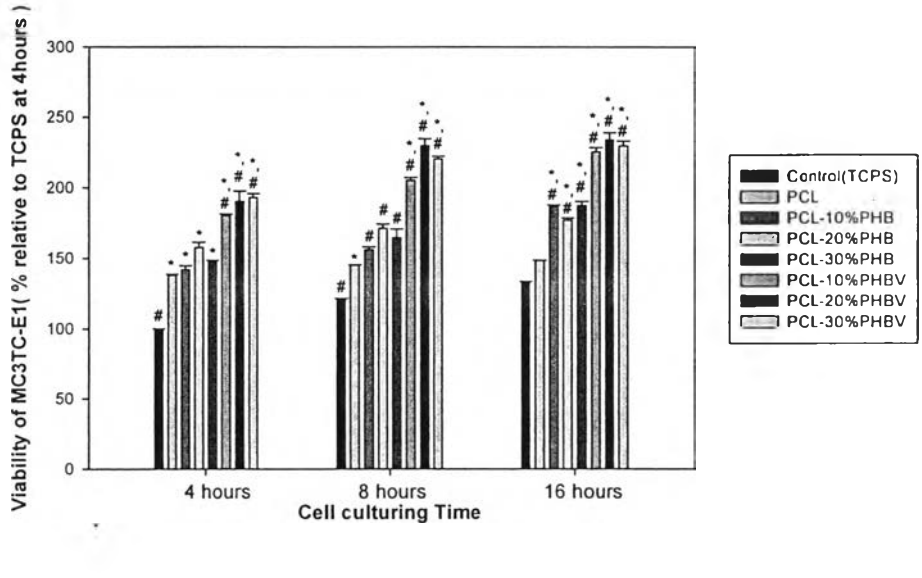

Figure 5.4 Attachment of MC3T3-E1 cells that were seeded or cultured on the surfaces of TCPS, PCL, PCL-10%PHB, PCL-20%PHB, PCL-30%PHB, PCL-10%PHBV, PCL-20%PHBV and PCL-30%PHBV dual-leached scaffolds for 4, 8, or 16 hours. Statistical significance: $^{*}p < 0.05$ compared with control and $^{\#}p < 0.05$ compared to the PCL scaffolds at any given time.

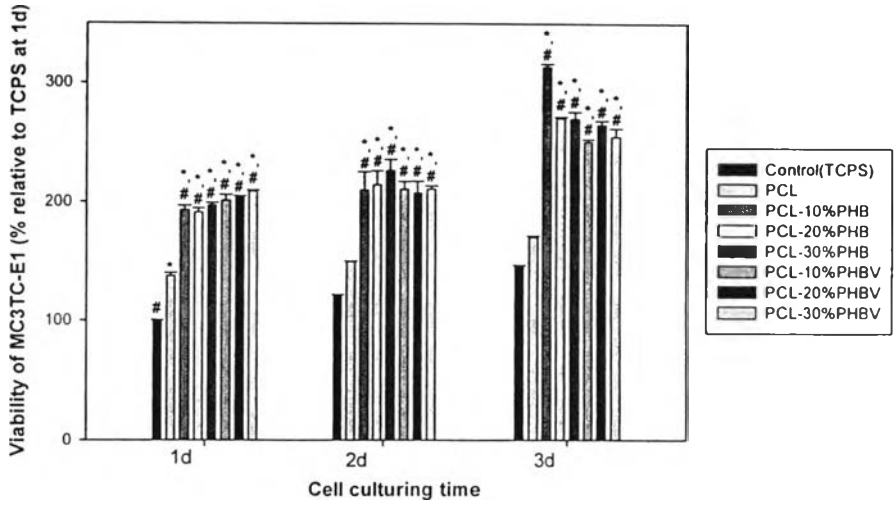

Figure 5.5 Proliferation of MC3T3-E1 cells that were seeded or cultured on the surfaces of TCPS, PCL, PCL-10%PHB, PCL-20%PHB, PCL-30%PHB, PCL-10%PHBV, PCL-20%PHBV and PCL-30%PHBV dual-leached scaffolds for 1, 2, or 3 days. Statistical significance: $^{*}p < 0.05$ compared with control and $^{\#}p < 0.05$ compared to the PCL scaffolds at any given time

Cell Morphology

Table 5.3 and 5.4 show selected SEM images (magnification = 3500X; scale bar = 5 μm) of MC3T3-E1 that were either seeded or cultured on the surfaces of glass, PCL, PCL-PHB, and PCL-PHBV dual-leached scaffolds at different time points. According to these images, cell morphology and interaction between cells and the scaffolds can be investigated. At 4 h after cells seeding, the majority of cells on the glass surface were stilled rounded and started to extend their cytoplasm. At 8 h after cells seeding, the majority of cells on the glass surface showed evidence of the extension of their cytoplasm on the surface. At 16 h after cells seeding, the majority of cells showed evidence of the expansion on the surface. For the cells that were seeded on the surface of all scaffolds, at 4 h after cells seeding, the majority of cells on surface showed evidence of the extension of their cytoplasm on the surface. At 8 h after cells seeding, the majority of cells showed evidence of the extension and expansion on the surface. At 16 h after cells seeding,

the majority of cells expanded over the area of scaffolds which were the most expansion on PCL-10%PHB, PCL-20%PHB, PCL-20%PHBV, and PCL-30%PHBV dual-leached scaffolds. At 1, 2, and 3 days after cells seeding, the majority of the cells seeded on the surfaces of all types of scaffolds expanded over the area of the scaffolds. The most expansion were on the surface of PCL-10%PHB dual-leached scaffold at any given time point.

Table 5.3 Attachment of MC3T3-E1 that had been seeded or cultured on the surfaces of glass, the PCL, the PCL-PHB and the PCL-PHBV dual-leached scaffolds for 4, 8, or 16 h. Selected SEM images of cultured specimens, i.e., glass (i.e., control), PCL, PCL-PHB, and PCL-PHBV dual-leached scaffolds at three different time points after MC3T3-E1 were seeded or cultured on their surfaces (magnification = 3500X; scale bar = 5 μm)

Culturing time		4h	8h	16h
Substrate	Glass	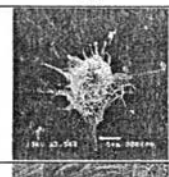	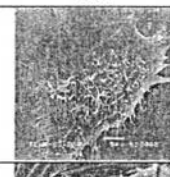	
	PCL		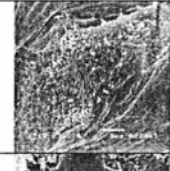	
	PCL-10% PHB			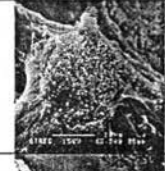
	PCL-20% PHB		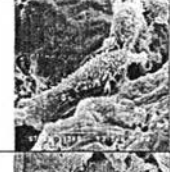	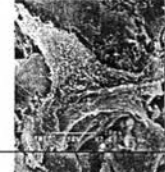
	PCL-30% PHB			
	PCL-10% PHBV	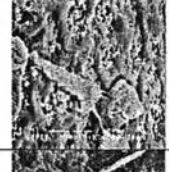	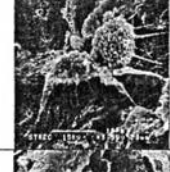	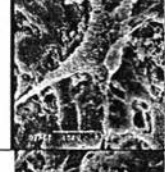
	PCL-20% PHBV		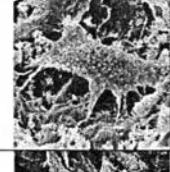	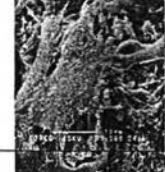
	PCL-30% PHBV			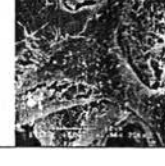

Table 5.4 Proliferation of MC3T3-E1 that had been seeded or cultured on the surfaces of the glass, the PCL, the PCL-PHB and the PCL-PHBV dual-leached scaffolds for 1, 2, or 3d. Selected SEM images of cultured specimens, i.e., glass (i.e., control), PCL, PCL-PHB, and PCL-PHBV dual-leached scaffolds at three different time points after MC3T3-E1 were seeded or cultured on their surfaces (magnification = 3500X; scale bar = 5 μm)

Culturing time		1d	2d	3d
Substrate	Glass	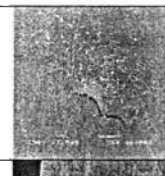	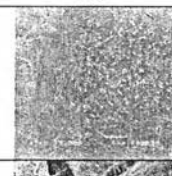	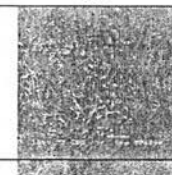
	PCL	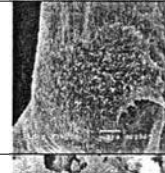	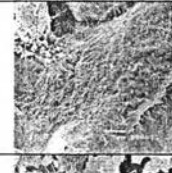	
	PCL-10% PHB			
	PCL-20% PHB			
	PCL-30% PHB		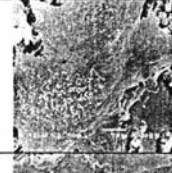	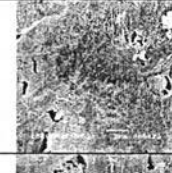
	PCL-10% PHBV	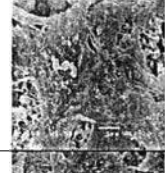	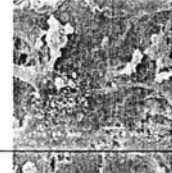	
	PCL-20% PHBV	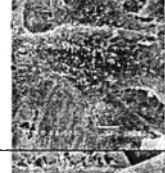	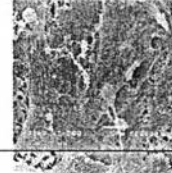	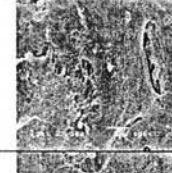
	PCL-30% PHBV		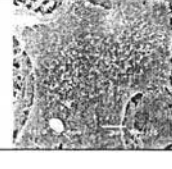	

Alkaline Phosphatase (ALP) Activity

Among the various biological functions of osteoblasts, secretion of alkaline phosphatase (ALP) is an important indicator determining the activity of the cells on a scaffold. The ALP activity of MC3T3-E1 cells that were cultured on PCL scaffolds for 3, 5, and 7 days. The ALP activity of MC3T3-E1 on TCPS (i.e. controls), PCL, PCL-PHB, and PCL-PHBV dual-leached scaffolds were monitored at 3, 5 and 7 days in culture (see Figure 5.6). For all of PCL-PHB and PCL-PHBV scaffolds investigated, the ALP activities were higher than TCPS on day 3 and 5 and were significantly higher than PCL at any given time point. Whereas the ALP activities on day 7 for PCL-PHB and PCL-PHBV were significantly higher than PCL but they were lower than TCPS. Since ALP activity is also detected in several non-calcified tissues and organs as the kidney, small intestines and placenta, it could be indicated that the ALP acitivity of MC3T3-E1 that were cultured on scaffolds could not be a marker of the calcification process.[43-46]

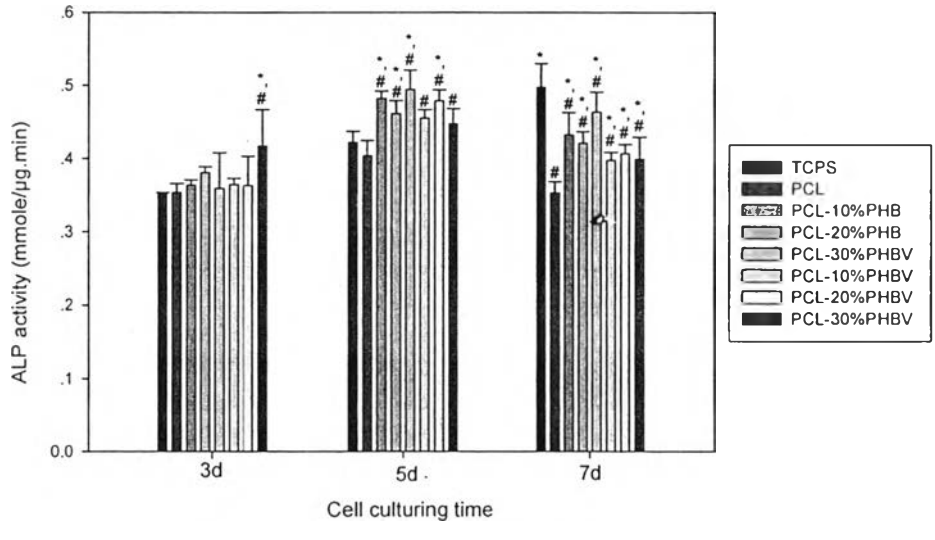

Figure 5.6 Alkaline phosphatase (ALP) activity of MC3T3-E1 cells that were cultured on the surfaces of TCPS, PCL, PCL-10%PHB, PCL-20%PHB, PCL-30%PHB, PCL-10%PHBV, PCL-20%PHBV and PCL-30%PHBV dual-leached scaffolds for 3, 5, or 7 days. Statistical significance: $^{*}p < 0.05$ compared with control and $^{\#}p < 0.05$ compared to the PCL scaffolds at any given time.

Mineralization

Alizarin Red S staining was used to quantify the mineral deposition of MC3T3-E1 that were cultured on the surfaces of TCPS, PCL, PCL-PHB, and PCL-PHBV dual-leached scaffolds for 14 and 21 days. Table 5.5 shows photographic images of the stained specimens. The appearance of red on the stained product shows the presence of calcium. In the presence of calcium, the Alizarin Red S-calcium chelating product appeared red. On day 14 after cell culturing, the red staining product observed for PCL-30%PHB dual-leached scaffolds was greatest, followed by that observed for PCL-20%PHB, and PCL-20%PHBV. An increase in the red staining product was observed for all the surfaces investigated on day 21. The quantitative analysis of the results shown in Figure 5.7 was carried out by elution of calcium deposition with cetylpyridinium chloride and spectrophotometically read at 570 nm. The extracted stain absorbance obtained on days 14 supported the above data where highest intensity of staining product was observed on PCL-30%PHBV, followed by PCL-30%PHB, PCL-20%PHB, and PCL-20%PHBV respectively. When the culture was maintained up to 21 days, significantly greater amount of calcium deposition were observed on PCL-PHB, and PCL-PHBV scaffolds compared to PCL scaffold and TCPS.

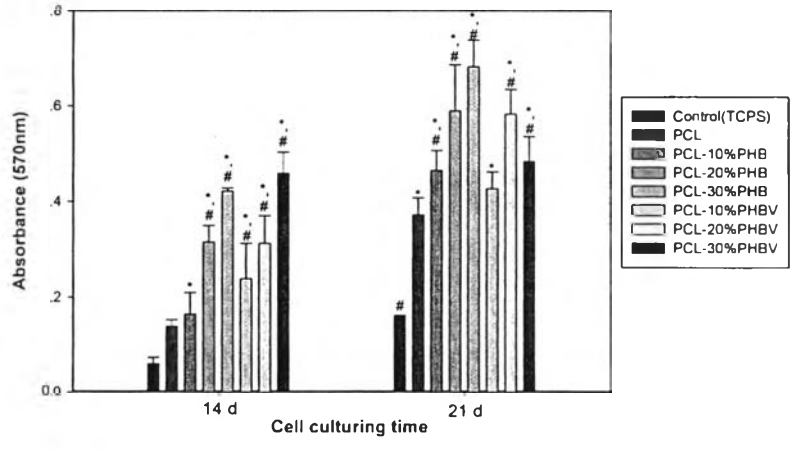

Figure 5.7 Quantification of mineral deposition in MC3T3-E1 cells by Alizarin Red-S staining. Statistical significance: $^{*}p < 0.05$ compared with control and $^{\#}p < 0.05$ compared to the PCL, the PCL-PHB, and the PCL-PHBV scaffolds at any given time point.

Table 5.5 Images of Alizarin Red-S staining for the mineralization in MC3T3-E1 on the TCPS, the PCL, the PCL-PHB, and the PCL-PHBV dual-leached scaffolds at 14 and 21 day

Substrate	Day			
	14 Day		21 Day	
	+ Cell	- Cell	+ Cell	-Cell
TCPS	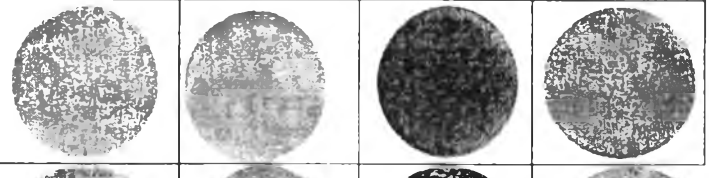			
PCL	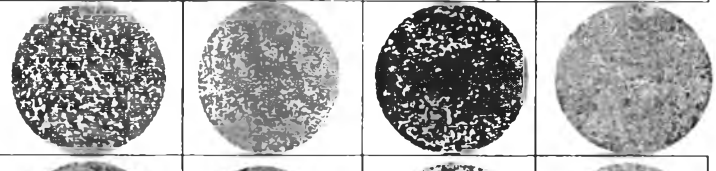			
PCL-10% PHB	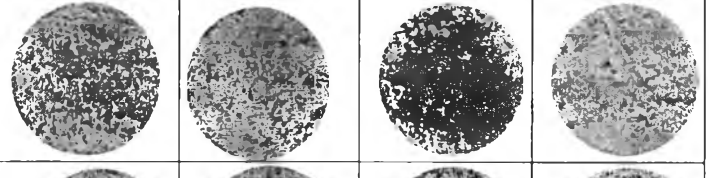			
PCL-20% PHB	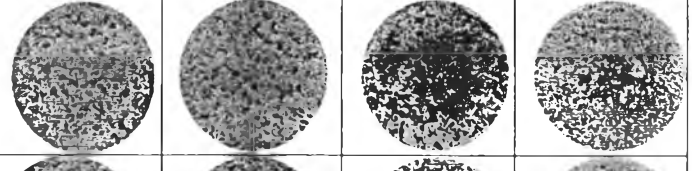			
PCL-30% PHB	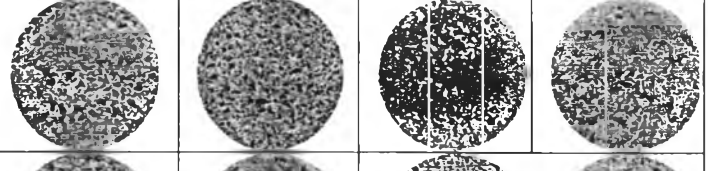			
PCL-10% PHBV	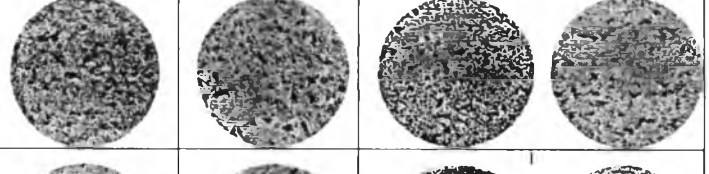			
PCL-20% PHBV	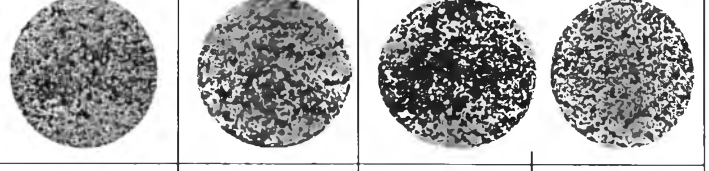			
PCL-30% PHBV	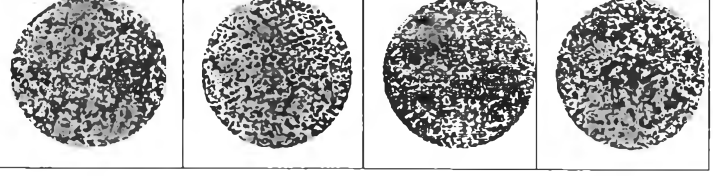			

5.5 Conclusion

PCL, PCL-PHB, and PCL-PHBV dual-leached scaffolds have been prepared by combining solvent casting and salt particulate leaching with polymer leaching technique. The PCL, PCL-PHB, and PCL-PHBV dual-leached scaffolds have been extensively characterized in terms of physical and mechanical properties such as morphology, compressive modulus, water absorption capacity, and remaining weight after degradation. The compressive modulus increased from ~ 58 kPa for the PCL scaffold to ~287 - 1,861 kPa for PCL-PHB and PCL-PHBV dual-leached scaffolds. Mechanical properties of PCL-PHB and PCL-PHBV dual-leached scaffolds have been greatly improved by blending of PHB or PHBV. For the degradation observation, the remaining weight of PCL, PCL-PHB and PCL-PHBV dual leached scaffolds were much decreasing compare to the absence of lipase condition. These results could be suggested that the activity of this enzyme lipase exhibited an effect to PCL, PCL-PHB, and PCL-PHBV dual leached scaffolds. Indirect cytotoxicity evaluation of these scaffolds with mouse fibroblastic cells (L929) and mouse calvaria-derived pre-osteoblastic cell (MC3T3-E1) indicated biocompatibility of these materials to both types of cell. The potential for use of these scaffolds as bone scaffolds was further assessed in vitro in terms of the attachment, the proliferation, the alkaline phosphatase (ALP) activity, and the mineralization of MC3T3-E1 that were seeded or cultured at different times. The obtained results showed that the both PCL-PHB and PCL-PHBV scaffolds exhibited better adhesion of cells than the TCPS and the PCL-PHB and PCL-PHBV dual-leached scaffolds exhibited better proliferation of cells than the corresponding TCPS and other scaffolds. Evidently, the cells that were cultured on all of the PCL-PHB and PCL-PHBV dual-leached scaffolds at 4 h appeared to be well-expanded and attach on scaffolds surface while that seeded on glass substrate was still in round shape. The cells that were cultured on PCL-10%PHB dual-leached scaffold showed the most expansion on the surface of scaffold. In mineralization assessment of MC3T3-E1 on days 14 and 21, the most intensity of staining product for calcium deposition were observed on PCL-PHB, and PCL-PHBV scaffolds compared to PCL

scaffold and TCPS. Our results indicate that PCL-PHB and PCL-PHBV dual-leached scaffolds possesses improvement in mechanical properties and degradation rate and its ability to support MC3T3-E1 cell attachment, proliferation, and mineralization for used as bone scaffolding material.

5.6 Acknowledgements

This work received partial financial support from 1) the Thailand Research Fund (TRF, grant no. DBG5280015 and a doctoral scholarship received from the Royal Golden Jubilee Ph.D. Program, PHD/0100/2551); 2) the "Integrated Innovation Academic Center: IIAC (RES_01_54_63)", Chulalongkorn University Centenary Academic Development Project, Chulalongkorn University; 3) the Petroleum and Petrochemical College (PPC), Chulalongkorn University; 4) the National Center of Excellence for Petroleum, Petrochemicals, and Advanced Materials, Thailand; and 5) the Department of Anatomy, Faculty of Dentistry, Chulalongkorn University.

5.7 References

[1] Amir, N. Ha., Hosseinalipour, S.M., Rezaie, H.R., and Shokrgozar, M.A. (2012) Characterization of poly(3-hydroxybutyrate)/nano-hydroxyapatite composite scaffolds fabricated without the use of organic solvents for bone tissue engineering applications. Materials Science and Engineering C, 32, 416–422

[2] Masami, O. and Baiju J. (2013) Synthetic biopolymer nanocomposites for tissue engineering scaffolds. Progress in Polymer Science, 38, 1487– 1503

[3] Rezwan, K., Chena, Q.Z., Blakera, J.J., and Aldo, R.B. (2006) Biodegradable and bioactive porous polymer/inorganic composite scaffolds for bone tissue engineering. Biomaterials, 27, 3413–3431

[4] Yung-Chih, K., and Cheng-Ting, W. (2012) Neuronal differentiation of induced pluripotent stem cells in hybrid polyester scaffolds with heparinized surface. Colloids and Surfaces B: Biointerfaces, 100, 9– 15

[5] Hutmacher, D.W. (2001) Scaffold design and fabrication technologies for engineering tissues--state of the art and future perspectives. Biomaterial Science Polymer Edition, 12 (1), 107-24

[6] Ilaria, C., Manuela, C., and Alessandra, B. (2013) Tailoring the properties of electrospun PHBV mats: Co-solution blending and selective removal of PEO. European Polymer Journal, 49, 3210–3222

[7] Long, Y., Katherine, D., and Lin, L. (2006) Polymer blends and composites from renewable resources. Progress in Polymer Science, 31, 576–602

[8] Perrine, B., Eric, P., and Luc, A. (2009) Nano-biocomposites: Biodegradable polyester/nanoclay systems. Progress in Polymer Science, 34, 125–155

[9] Joel, R., and Michel, A. H. (2006) Preparation of interconnected poly(ε-caprolactone) porous scaffolds by a combination of polymer and salt particulate leaching. Polymer, 47, 4703–4717

[10] Prae-ravee, K., Prasit, P., and Pitt, S. (2011) Effect of the Surface Topography of Electrospun Poly(ε-caprolactone)/Poly(3-hydroxybuterate-co-3-hydroxyvalerate) Fibrous Substrates on Cultured Bone Cell Behavior. Langmuir, 27, 10938–10946

[11] Lida, B. H., Yashchuk, O., and Miyazaki, S.S. (2009) Changes in the mechanical properties of compression moulded samples of poly(3-hydroxybutyrate-co-3-hydroxyvalerate) degraded by Streptomyces omiyaensis SSM 5670E′. Polymer Degradation and Stability, 94, 267–271

[12] Jian, T., Cunjiang, S., Mingfeng, C., Dan, H., Li, L., Na, L., and Shufang, W. (2009) Thermal properties and degradability of poly(propylene carbonate)/poly(b-hydroxybutyrate-co-b-hydroxyvalerate) (PPC/PHBV) blends. Polymer Degradation and Stability, 94, 575–583

[13] Marrakchi, Z., Oueslati, H., Belgacem, M.N., Mhenni, F., and Mauret, E. (2012) Biocomposites based on polycaprolactone reinforced with alfa fibre mats. Composites: Part A, 43, 742–747

[14] Lijun, J., Wenjun, W., Duo, J., Songtao, Z., and Xiaoli, S. (2015) In vitro bioactivity and mechanical properties of bioactive glass nanoparticles/polycaprolactone composites. Materials Science and Engineering C, 46, 1–9

[15] Rezwan, K., Chena, Q.Z., Blakera, J.J., and Aldo, R.B. (2006) Biodegradable and bioactive porous polymer/inorganic composite scaffolds for bone tissue engineering. Biomaterials, 27, 3413–3431

[16] Xian-Yi, X., Xiao-Tao, L., Si-Wu, P., Jian-Feng, X., Chao, L., Guo, F., Kevin, C. C., and Guo-Qiang, C. (2010) The behaviour of neural stem cells on polyhydroxyalkanoate nanofiber scaffolds. Biomaterials, 31, 3967–3975

[17] Donghua, G., Zhiqing, C., Chunpeng, H., and Yinghe, L. (2008) Attachment, proliferation and differentiation of BMSCs on gas-jet/electrospun nHAP/PHB fibrous scaffolds. Applied Surface Science, 255, 324–327

[18] Shuai, W., Piming, M., Ruyin, W., Shifeng, W., Yong, Z., and Yinxi, Z. (2008) Mechanical, thermal and degradation properties of poly(d,l-lactide)/poly(hydroxybutyrate-co-hydroxyvalerate)/poly(ethylene glycol) blend. Polymer Degradation and Stability, 93, 1364–1369

[19] Sanaz, A., Samira, S., Nor Azowa, I., Wan, M. Z., Wan, Y., Mohamad, Z. A. R., Susan, A., and Asma, F. (2012) Enhancement of Mechanical and Thermal Properties of Polycaprolactone/Chitosan Blend by Calcium Carbonate Nanoparticles. International Journal of Molecular Science, 13, 4508-4522

[20] Shaun, E. and Suman, D. (2010) Mechanical and microstructural properties of polycaprolactone scaffolds with one-dimensional, two-dimensional, and three-dimensional orthogonally oriented porous architectures produced by selective laser sintering. Acta Biomaterialia, 6, 2467–2476

[21] MyllymaÈ, K.O., MyllaÈ, R.P., Forssell, P., Suortti, T., LaÈ hteenkorva, K., Ahvenainen, R., and Poutanen, K. (1998) Mechanical and Permeability Properties of Biodegradable Extruded Starch/polycaprolactone Films. PACKAGING TECHNOLOGY AND SCIENCE, 11, 265-274

[22] Ken-Jer, W., Chin-San, W., and Jo-Shu, C. (2007) Biodegradability and mechanical properties of polycaprolactone composites encapsulating phosphate-solubilizing bacterium Bacillus sp. PG01. Process Biochemistry, 42, 669–675

[23] Chern, C. E., Nor, A. I., Norhazlin, Z., Hidayah, A.,Wan, Md., Zin, W. Y., Yoon, Y. T., and Cher, C. T. (2013) Enhancement of Mechanical and Thermal Properties of Polylactic Acid/Polycaprolactone Blends by Hydrophilic Nanoclay. Indian Journal of Materials Science, 11

[24] Korakot, S., Neeracha, S., Prasit, P., and Pitt, S. (2007) Bone scaffolds from electrospun fiber mats of poly(3-hydroxybutyrate), poly(3-hydroxybutyrate-co-3-hydroxyvalerate) and their blend. Polymer, 48, 1419-1427

[25] Chuan, Y., Ping, H., Min-Xian, M., Yang, X., Ri-Guang, L., and Xian-Wen, S. (2009) PHB/PHBHHx scaffolds and human adipose-derived stem cells for cartilage tissue engineering. Biomaterials, 30, 4401–4406

[26] Zhao, K., Deng, Y., and Chen, G.Q. (2003) Effects of surface morphology on the biocompatibility of polyhydroxyalkanoates. Biochemical Engineering Journal, 16, 115–123

[27] Johari, N., Fathi, M.H., and Golozar, M.A. (2012) Fabrication, characterization and evaluation of the mechanical properties of poly(ε-caprolactone)/nano-fluoridated hydroxyapatite scaffold for bone tissue engineering. Composites: Part B, 43, 1671-1675

[28] Murali, M. R., Singaravelu, V., Manjusri, M., Sujata, K. B., and Amar, K. M. (2013) Biobased plastics and bionanocomposites: Current status and future opportunities. Progress in Polymer Science, 38, 1653– 1689

[29] Chunyan, Z., Aaron, T., Giorgia, P., and Han, K. H. (2013) Nanomaterial scaffolds for stem cell proliferation and differentiation in tissue engineering. Biotechnology Advances, 31, 654–668

[30] Christina, W. C., Loran, D. S., and Eben, A. (2014) Decellularized tissue and cell-derived extracellular matrices as scaffolds for orthopaedic tissue engineering. Biotechnology Advances , 32, 462–484

[31] Kai, Z., Ying, D., Jin, C. C., and Guo-Qiang, C. (2003) Polyhydroxyalkanoate (PHA) scaffolds with good mechanical properties and biocompatibility. Biomaterials, 24, 1041–1045

[32] Orawan, S., Suchada, W., Neeracha, S., Prasit, P., Poonlarp, C., Tanom, B., and Pitt, S. (2007) In vitro biocompatibility of electrospun poly(3-hydroxybutyrate) and poly(3-hydroxybutyrate-co-3-hydroxyvalerate) fiber mats. International Journal of Biological Macromolecules, 40, 217–223

[33] Thadavirul, N., Pavasant, P., and Supaphol, P. (2013) Development of polycaprolactone porous scaffolds by combining solvent casting, particulate

leaching, and polymer leaching techniques for bone tissue engineering. Journal of Biomedical Material Research Part A, 00A, 000-000

[34] Thadavirul, N., Pavasant, P., and Supaphol, P. (2014) Improvement of dual-leached polycaprolactone porous scaffolds by incorporating with hydroxyapatite for bone tissue regeneration. Journal of Biomaterials Science, Polymer Edition, 0,000-000

[35] Shor, L., Cuceri, S., Wen, X., Gandhic, M., and Suna, W. (2007) Fabrication of three-dimensional polycaprolactone/hydroxyapatite tissue scaffolds and osteoblast-scaffold interactions in vitro. Biomaterial, 28, 5291-5297

[36] Liu, C., Xia, Z., and Czernuszka, J.T. (2007) Design and Development of Three-Dimensional Scaffolds for Tissue Engineering. Chemistry Engineering Research Des, 85, 1051-1064

[37] Wei, G., and Ma, P.X. (2004) Structure and properties of nano-hydroxyapatite/polymer composite scaffolds for bone tissue engineering. Biomaterial, 25, 4749-4757

[38] Yang, F., Cui, W., Xiong, Z., Liu, L., Bei, J., and Wang, S. (2006) Poly(L,L-lactide-co-glycolide)/ tricalcium phosphate composite scaffold and its various changes during degradation in vitro. Polymer Degradation Stability, 91, 3065-3073

[39] Webster, T.J., Ergun, C., Doremus, R.H., Siegel, R.W., and Bizios, R. (2000) Enhanced functions of osteoblasts on nanophase ceramics. Biomaterial, 21, 1803-1810